

1 ***In silico* homology modelling and identification of Tousled-like kinase 1**
2 **inhibitors for glioblastoma therapy via high throughput virtual screening**
3 **protein-ligand docking**

4
5 Kamariah Ibrahim¹

6 Abubakar Danjuma²

7 Chyan Leong Ng³

8 Nor Azian Abdul Murad¹

9 Roslan Harun^{1, 4}

10 Wan Zurinah Wan Ngah^{1, 5}

11 and *Rahman Jamal^{1,5}

12

13 ¹UKM Medical Molecular Biology Institute (UMBI), National University of Malaysia,
14 Cheras, Jalan Yaacob Latiff, Bandar Tun Razak, 56000, Cheras, Kuala Lumpur, Malaysia

15 ²Kulliyyah of Pharmacy, International Islamic University Malaysia, Jalan Sultan Ahmad
16 Shah, Bandar Indera Mahkota, 25200 Kuantan, Pahang Darul Makmur

17 ³Institute of Systems Biology, National University of Malaysia, 436000, Bangi,

18 ⁴KPJ Ampang Puteri Specialist Hospital, Jalan Memanda 9, Taman Dato Ahmad Razali,
19 68000 Ampang, Selangor, Malaysia

20 ⁵Faculty of Medicine, National University of Malaysia, 56000, Cheras, Kuala Lumpur

21

22 ***Corresponding author:**

23 Rahman Jamal

24 Address: UKM Medical Molecular Biology Institute (UMBI), National University of

25 Malaysia, Jalan Yaacob Latiff, Bandar Tun Razak, 56000, Cheras, Kuala Lumpur

26 Email: rahmanj@ppukm.ukm.edu.my

27 **Phone: +603-91456321/9239**

28 **Fax: +603-91717185**

29

30 **Acknowledgements:** This study was funded by the Higher Institution Centre of Excellence

31 (HICoE) research grant (JJ-015-2011), Ministry of Education, Malaysia

32

33 **Conflicts of interest:** All members declare no conflict of interest

34

35 **Keywords:** Tausled-like kinase 1, TLK1, GBM, Homology modelling, *in silico* high

36 throughput virtual screening

37

38

39

40

41

42 **Abstract**

43 **Background:** Glioblastoma multiforme (GBM) is a grade IV brain tumor that arises from star-
44 shaped glial cells supporting neural cells called astrocytes. The survival of GBM patients
45 remains poor despite many specific molecular targets that have been developed and used for
46 therapy. Tausled-like kinase 1 (TLK1), a serine-threonine kinase, was identified to be
47 overexpressed in cancers such as GBM. TLK1 plays an important role in controlling
48 chromosomal aggregation, cell survival and proliferation. *In vitro* studies suggested that TLK1
49 is a potential target for some cancers; hence, the identification of suitable molecular inhibitors
50 for TLK1 is warranted as a new therapeutic agents in GBM. To date, there is no structure
51 available for TLK1. In this study, we aimed to create a homology model of TLK1 and to
52 identify suitable molecular inhibitors or compounds that are likely to bind and inhibit TLK1
53 activity via *in silico* high-throughput virtual screening (HTVS) protein-ligand docking.

54 **Methods:** 3D homology models of TLK1 were derived from various servers including
55 HOMology Modeller, i-Tasser, Psipred and Swiss Model. All models were evaluated using
56 Swiss Model Q-Mean server. Only one model was selected for further analysis. Further
57 validation was performed using PDBsum, 3d2go, ProSA, Procheck analysis and ERRAT.
58 Energy minimization was performed using YASARA energy minimization server.
59 Subsequently, HTVS was performed using Molegro Virtual Docker 6.0 and candidate ligands
60 from ligand.info database. Ligand-docking procedures were analyzed at the putative catalytic
61 site of TLK1. Drug-like molecules were filtered using FAF-Drugs3, which is an ADME-Tox
62 filtering program. **Results and conclusion:** High quality homology models were obtained from
63 the Aurora B kinase (PDB ID:4B8M) derived from *Xenopus levius* structure that share 33%
64 sequence identity to TLK1. From the HTVS ligand-docking, two compounds were identified
65 to be the potential inhibitors as it did not violate the Lipinski rule of five and the CNS-based
66 filter as a potential drug-like molecule for GBM.

67 **Background**

68 Glioblastoma multiforme (GBM) is the most common primary brain tumor in adults. It is also
69 classified as grade IV glioma which arises from the lineage of star-shaped glial cells known as
70 astrocytes. The survival rate is very poor where only 15% of patients survived more than 24
71 months due to disease aggressiveness and heterogeneity of the disease (Ohgaki, & Kleihues
72 2007; Ohgaki et al. 2004). Although several molecular inhibitors have been developed to target
73 aberrantly expressed enzymes and proteins, the results have been very frustrating (Li, & Tu
74 2015; Piccirillo et al. 2015). Factors contributing to resistant of GBM cells include deregulation
75 of key signalling pathways, namely *PTEN*, *TP53*, *RB* and *PI3K-Akt* (Ohgaki, & Kleihues 2011;
76 Smith et al. 2001), increased in the expression of anti-apoptotic proteins *BCL2* and *survivin*
77 (Guvenc et al. 2013; Ruano et al. 2008), iterative perivascular growth within the highly
78 vascularized brain (Baker et al. 2014), and presence of 30-65% constitutively active *EGFRvIII*
79 mutant in GBM which secretes higher levels of invasion-promoting proteins (Sangar et al.
80 2014). Studies have revealed that Tausled-like kinase 1 (*TLK1*) is overexpressed in breast
81 cancer (Wolfort et al. 2006), prostate cancer (Ronald et al. 2011), and cholangiocarcinoma
82 (Takayama et al. 2010). In our previous study, we proved that *TLK1* is overexpressed in GBM
83 and silencing of *TLK1* results in a significant decrease in invasion, migration and GBM cells
84 survival (Ibrahim et al. 2013).

85

86 Human TLK1 contains 766 amino acids and is one of the members of the Tausled-like kinase
87 family consisting of TLK1 and TLK2 (Pruitt et al. 2012). The gene is mapped on chromosome
88 2q31.1 and encoded by 25 exons. TLK1 share 85% sequence identity to TLK2, and both share
89 ~50% sequence identity with *Arabidopsis thaliana* where Tausled-like kinase family was
90 initially identified (Takahata, Yu & Stillman 2009). This serine-threonine kinase is an
91 important signalling regulator mainly involved in the cell cycle regulation, cellular mitosis, cell

92 survival, and proliferation (Sunavala-Dossabhoy, & De Benedetti 2009). In general, the N-
93 terminal domain of Tousled-like kinase is well conserved to include three potential nuclear
94 localization sequences and three putative coiled-coil regions, while the C-terminus region
95 contains the catalytic ATP-binding domain at the region that consists of 456 to 734 amino acid
96 residues. The active binding site is located within the protein kinase domain sequence (Silljé
97 et al. 1999). This ~90 kDa kinase is activated by the *CHK1/ATM DNA* damage pathway (Groth
98 et al. 2003). TLK1 interacts with its substrates, namely Asf1, histone H3 (Carrera et al. 2003),
99 and Rad9 (Sunavala-Dossabhoy, & De Benedetti 2009) to activate DNA damage and DNA
100 repair activity (De Benedetti 2012). It was suggested that when overexpressed, *TLK1* is
101 involved in radioprotection and chemo-resistance of cancer cells (Y. Li et al. 2001; Ronald et
102 al. 2011). Unfortunately, the structure of TLK1 has not been elucidated and this hinders the
103 full understanding of TLK1 biological processes. Nonetheless, the X-ray diffraction data for
104 the kinase domain of human TLK1 family member TLK2 have been recently reported which
105 may shed a light on structural understanding of human Tousled-like kinase (Garrote et al.
106 2014). No structure is yet available for both TLK1 and TLK2, hence, we perform a homology
107 modelling study of TLK1 structure to understand its function in orchestrating cellular functions
108 particularly in cancer pathways. In this study, we present a structural homology model of the
109 TLK1 catalytic binding domain which may serve as a potential target for molecular inhibitors.
110 We then used the proposed structure to identify potential inhibitors for TLK1 by utilising *in*
111 *silico* ligand-docking with high throughput virtual screening (HTVS) targeting more than
112 16,000 candidate compounds.

113

114

115

116 Materials and methods**117 Template identification and homology modelling**

118 The amino acid sequence of human TLK1 was retrieved from UniProt with the accession
119 number: Q9UKI8 (<http://www.uniprot.org/>). The TLK1 FASTA format amino acid sequence
120 was downloaded into the BLASTP and PSI-BLAST search (<http://blast.ncbi.nlm.nih.gov/>) in
121 order to identify the homologous proteins. An appropriate template for TLK1 was identified
122 based on the e-value and sequence identity ranging from 30% to 33% at the protein kinase
123 domain indicating similarity of structure and function. The template and the target sequences
124 were later aligned using the Clustal Omega program
125 (<http://www.ebi.ac.uk/Tools/msa/clustalo/>). Subsequently, homology modelling was carried
126 out against the chosen template using HOMology Modeller (Tosatto 2005), I-Tasser (Zhang
127 2009), and PsiPred (Buchan et al. 2010).

128

129 Homology models quality estimation

130 The model quality estimation was performed using the Swiss-Model Qualitative Model Energy
131 Analysis (Q-Mean) Server based on the composite scoring function, which derives a quality
132 estimation on the basis of the geometrical analysis of single models (Benkert, Biasini &
133 Schwede 2011). It also describes the major geometrical aspects of the protein structures. Five
134 different structural descriptors were used. The local geometry was analyzed using the torsion
135 angle potential function over three consecutive amino acids. A secondary structure-specific
136 distance-dependent pairwise residue-level potential was used to assess long-range interactions.
137 A solvation potential describes the burial status of the residues. Two simple terms describing
138 the agreement of predicted and calculated secondary structure and solvent accessibility, were
139 also included. In comparison with other protein structure evaluation servers, the QMEAN

140 shows a statistically significant improvement over nearly all quality measures describing the
141 ability of the scoring function to identify the native structure and to discriminate good from
142 bad models (Benkert, Tosatto & Schomburg 2008). 3D structure was then visualized using
143 PyMol software (The PyMOL Molecular Graphics System, Version 1.5.0.4 Schrödinger,
144 LLC).

145

146 **Validation of modelled structure**

147 The best homology model created was used for further investigation. We used the latest version
148 of PDBsum (<http://www.ebi.ac.uk/thornton-srv/databases/pdbsum/>) which provides further
149 information on protein function prediction, structural topology, PROCHECK and cleft
150 analysis. We also used ProSA which displays scores and energy plots that highlight potential
151 problems spotted in protein structures (Wiederstein, & Sippl 2007). Prediction of the protein
152 structure function was performed using proteo-genomic analysis software 3d2go
153 (<http://www.sbg.bio.ic.ac.uk/phyre/pfd/html/help.html>). This allowed full structural scan of
154 the protein structure made against the Structural Classification of Proteins (SCOP) database
155 using a modified version of BLAST (Tung, Huang & Yang 2007). Energy minimization was
156 performed on YASARA server (<http://www.yasara.org/minimizationserver.php>).

157

158 **High throughput *in silico* ligand-docking analysis**

159 *In silico* ligand-docking analysis was performed using Molegro Virtual Docker (MVD version
160 2013.6.0) to predict protein-ligand interactions. The potential binding sites of selected proteins
161 and candidate small molecules were characterized by the molecular docking algorithm called
162 MolDock which was derived from “*Piecewise Linear Potential* (Sundarapandian et al. 2010).
163 The MolDock score refers to the approximate binding energies between protein and ligand

164 which is usually expressed in kcal/mol. This software handles all aspects of the docking
165 process from the preparation of the molecules to determine the potential binding site of the
166 target protein, and the predicted binding modes of the ligand. Interestingly, MVD has been
167 shown to provide higher accuracy compared with the other commercially available docking
168 softwares e.g. Glide, Surflex and FlexX (Sivaprakasam, Tosso & Doerksen 2009). Docking
169 requires five steps; importing molecules, importing ligands, molecular preparation, creating
170 template and docking.

171

172 Candidate ligands for ligand-docking screening were downloaded from Ligand.Info
173 (<http://ligand.info/>) which compiles various publicly available databases of small molecules
174 and compounds from ChemBank, KEGG, ChemPDB, Drug-likeness NCI subset and non-
175 annotated NCI subset (von Grotthuss, Pas & Rychlewski 2003). We downloaded a total of
176 16,358 sdf. format small molecules from KEGG ligands (10,005), ChemBank (2,344) and
177 ChemPDB (4,009) for high throughput screening of potential inhibitors for TLK1. Due to the
178 large number of candidate KEGG ligands, we filtered out some of these compounds based on
179 the relevancy to the present TLK1 3D model using Findsite server (Brylinski, & Skolnick 2008)
180 as a pre-molecular docking step. After filtering these ligands, only 1,386 KEGG ligands were
181 selected for further investigation. Most of the ligands in the database as well as the homology
182 model or molecule did not have correct bond orders and bond angles. Hence, full optimization
183 of molecules and ligand preparation was performed using Molegro Virtual Docking software
184 default setting whereby appropriate missing hydrogen atoms were added, missing bonds were
185 assigned, partial charges were added if necessary and flexible torsions in ligands detected.

186

187 Docking study was performed at the catalytic domain of TLK1. Simulation on the modelled
188 protein identified five cavities as potential binding sites. However, only one cavity was used
189 for the ligand-docking study i.e. the cavity with the largest surface area and volume of 214.528
190 arbitrary unit within the catalytic domain sites of TLK1. The predicted sites had a grid resolution
191 of 0.3Å and a binding site of 15Å radius from the template. The Moldock optimizer was used
192 as a search algorithm and the number of runs was set to 10 with a maximum iteration of 1000,
193 scaling factor of 0.50, 0.90 cross over and a population size of 50. The maximum number of
194 poses generated was 5. Potential ligands were selected based on the best MolDock score value
195 that is less than -170.

196

197 **Visualization of ligand-protein interaction**

198 The three-dimensional and two-dimensional visualisation of ligand-protein interaction were
199 performed using the Maestro software package (Maestro, version 10.4, Schrödinger, LLC, New
200 York, NY, 2015).

201

202 ***In silico* bioavailability study**

203 Lead molecules identified from the high throughput ligand-docking screening were subjected
204 to further *in silico* filtering to identify those with the best values in terms of their absorption,
205 distribution, metabolism, excretion and toxicity (ADME-Tox). This was done using the FAF-
206 Drugs3 (November 2014 edition) which is a free ADME-Tox (Miteva et al. 2006) filtering tool.
207 This step will ensure the suitability of lead molecules based on toxicity for future *in vivo*
208 applications. We applied Lipinski's Rule of Five (Lipinski et al. 2001) to remove some reactive
209 groups and compounds. We have also included the Central Nervous System (CNS) drugs
210 physicochemical criteria (Jeffrey, & Summerfield 2010; Pajouhesh, & Lenz 2005), which

211 includes (1) molecular mass less than 450 Da, (2) partition coefficient (logP) of 0.2 -6.0, (3)
212 hydrogen bond donors not less than three, (4) hydrogen bond acceptors not less than five and
213 (5) topological surface area (tPSA) within 3-118.

214

215 **Results**

216 **Homology modelling of TLK1 serine/threonine kinase**

217 The PSI-BLAST results of TLK1 sequence Q9UKI8 were analysed and we selected the protein
218 hits based on query coverage, similarity and identity. The model structure which was selected
219 showed sequence identity and similarity that ranged from 27% to 37% and a query coverage
220 E-value that ranged from 4e-29 to 9e-15 and covered only the protein kinase domain site (450-
221 756). The homology model was created based on the TLK1 protein kinase catalytic domain
222 sequence. We selected 40 protein sequence templates for homology modelling using various
223 softwares. However, only 18 models were successfully created using HOMology Modeller
224 and i-tasser. We evaluated all the 18 models using Q-Mean Server and identified the Aurora B
225 kinase structure from African clawed frog *Xenopus levi* (PDB ID: 4B8M) as the best
226 template structure for TLK1 producing a Total QMean Score of 0.68 out of 1.0 required for an
227 excellent homology model (**Table 1**). The Aurora B kinase that in complex with inner
228 centromere protein A (VX-680) was determined to 1.85 Å resolution (PDB ID: 4B8M). Pro-
229 Motif analysis showed that the modelled TLK1 structure, with 270 amino acids, contains 4
230 beta-hairpins, 6-beta bulges, 10 strands, 14 helices, 15 helix-helix interactions, 16 beta-turns
231 and 3 gamma turns (**Figure 1A and 1B**).

232

233 The homology model of TLK1 was also assessed using ProSA Z-score. The overall Z-score
234 quality was -4.92 suggesting a good quality model compared with the available structure from

235 NMR and X-ray (**Figure 2A and 2B**). Ramachandran plot obtained from PROCHECK analysis
236 achieved a good quality model assessment of 90.1% in the favoured region (**Figure 2C**). The
237 plot represents the *psi* and the *phi* angles of the amino acid residues. Details of the analysis plot
238 can be referred to **Table 2**. Analysis from the three dimensional structural superposition (3d-
239 ss) web server (Sumathi et al. 2006) showed the root mean square deviation (RMSD) between
240 template structure and the 3D homology model structure to be 0.543 Å (**Figure 2D**). ERRAT
241 overall quality factor is 53.696% and at least more than 80% of the amino acids have scores
242 more than or equal to 0.2 in the 3D/1D profile. The YASARA public server for energy
243 minimization provided a value of 16140271100.5 kJ/mol to 143790.2 kJ/mol with a score of -
244 1.53 to -0.95.

245

246 **Proteogenomic analysis**

247 Functional analysis of the TLK1 modelled structure performed using 3d2go web server
248 identified the following activities with the highest confidence value of 1.0: phosphotransferase
249 activity alcohol group as the acceptor, protein amino acid phosphorylation, protein
250 serine/threonine kinase activity and nucleotide binding. Nucleus and protein binding functions
251 were predicted with a confidence value of 0.89. Functional prediction in cell cycle, mitosis,
252 phosphoinositide-mediated signalling (confidence value of 0.86), centrosome, spindle
253 organization, regulation of protein stability, ubiquitin protein ligase binding (confidence value
254 of 0.85) were all in concordance with experimental data (Kelly, & Davey 2013; Pilyugin et al.
255 2009). These findings were predicted to be similar with the function of human Aurora kinase2
256 (PDB ID: 2J4Z). Interestingly, with a confidence value of 0.79, the modelled TLK1 structure
257 is also predicted to be involved in insulin receptor signalling pathway and actin cytoskeleton
258 organization which is similar to the human PDK1 (PDB ID:1UU3). This indicates that TLK1

259 could be involved in the regulation of actin filament organization particularly in controlling
260 cancer cell motility.

261

262 **High throughput virtual ligand-docking screening**

263 The cut-off point of the MolDock docking scoring was set at less than -170 to select ligands
264 that predicted to have high binding affinity to TLK1. We identified 192 lead molecules, and
265 ATP was the top scoring molecule in the docking procedure with a MolDock score of -193.654.
266 The amino acid residues that found to involve in the protein-ligand interactions were GLY463,
267 ARG464, GLY465, GLY466, PHE467, SER468, GLU469, VAL470 and LYS485. The
268 compounds that utilized in the screening were initially not known until we have completed the
269 identification procedure. The results showed that ATP docked accurately within the cavity,
270 suggesting the robustness of the *in silico* experiment.

271

272 ***In silico* pharmacokinetic analysis**

273 The 192 compounds with the best MolDock scores were submitted to the Free ADME-Tox
274 filtering tool 3 (November 2014 edition) for pharmacokinetic analysis. Analysis were subjected
275 to the Lipinski's Rule of Five (RO5) (Lipinski et al. 2001) and filters for CNS drugs (Jeffrey,
276 & Summerfield 2010; Pajouhesh, & Lenz 2005) to ensure the efficacy and safety of the
277 candidate compounds. The final filtering process revealed that only two compounds passed this
278 assessment without violating the general Lipinski's RO5 and the CNS rule. These compounds
279 were identified as ID352 and ID1652 from the ChemBank database (**Table 3**). Their chemical
280 structures, IUPAC names, the radar plot of physicochemical analysis, oral absorption
281 estimation data and the Pfizer 3/75 Rule Positioning plot, which estimated drug-like molecules
282 that are likely to cause toxicity and experimental promiscuity, are presented in **Figure 3A-H**.

283 ID1652 is known as beraprost which is a prostacyclin analogue used in the treatment of arterial
284 hypertension (Galiè et al. 2002). It has a better docking score, with no violation of Lipinski's
285 rule of five and a low promiscuous toxicity as compared to ID352 or bepridil which is a calcium
286 channel blocker for anti-angina (Rae et al. 1985). Beraprost also has a better hydrogen bonding
287 score from the ligand-docking simulation. Results from receptor-ligand interactions (**Figure 4**)
288 revealed a common cavity for ATP, ID352 and ID1652 binding. The residues that are involved
289 in the interactions include GLY465, GLY466, PHE467, SER468, VAL470, and LYS485.
290 These suggested that both of the two compounds bind to catalytic site of TLK1 ATP binding
291 pocket.

292

293 Discussion

294 GBM remains as the solid tumour with the poorest survival in adults since the past few decades.
295 The search for the right molecular target is still ongoing and one of the many approaches is by
296 using computer-aided drug discovery tools. Our recent *in vitro* study identified TLK1 as a
297 potential target for glioblastoma multiforme. We found *TLK1* to be overexpressed and the
298 knockdown of *TLK1* reduced cellular proliferation and invasion (Ibrahim et al. 2013). An auto-
299 phosphorylated chemical inhibition screen on recombinant TLK1B, which is a known splice
300 variant, has been performed by Ronald et al, using more than 6,000 compounds. This study
301 identified four inhibitors belonging to the class of phenothiazine antipsychotics that are
302 structurally and chemically similar. The same study also showed that thioridazine was able to
303 sensitize prostate cancer cells when used with doxorubixin (Ronald et al. 2013). Although
304 chemical library screening for drug discovery seems promising, it is very expensive and time
305 consuming. A study using the ChemBL database and Kinase SaRfari application identified 74
306 "hits" compounds that can potentially bind to TLK1 (Bento et al. 2014). However, no details

307 were reported on the specific binding sites and the specific TLK1 structure that were used for
308 the screen. In this study we used a computational approach to identify suitable TLK1 inhibitors
309 based on a homology model that has been created.

310

311 The 3D structure of TLK1 is currently not available for drug design strategy, hence we used
312 18 PDB templates that shared 30% to 33% sequence identity, to create homology models of
313 TLK1. As a result, Aurora B kinase (PDB ID: 4B8M) was identified as the most suitable
314 homology template by the HOMology modeller server. This model allows us to perform
315 ligand-docking analysis to identify potential inhibitors for TLK1.

316

317 One of the major challenges for optimal therapeutic intervention for glioblastoma and other
318 types of brain tumor is to achieve maximal penetration across the blood brain barrier (BBB).
319 The BBB is a structure composed of endothelial cells which is associated with perivascular
320 neurons, pericytes and astrocytic end-feet processes. The endothelial cells connected by tight
321 junctions form an almost impenetrable barrier to all compounds except highly lipidized small
322 molecules of less than 400 Da (Nathanson, & Mischel 2011). Although many studies have
323 identified drug-like molecules from high throughput virtual screening, most only follow the
324 Lipinski's rule of five and have neglected the probability calculations for the molecules to cross
325 the BBB. This eventually led to dismal results in *in vivo* studies (Gidda et al. 1995; Pardridge
326 1998). We used the recent version of the free ADME-TOX software and utilized the CNS filter
327 to identify drug-like molecules that are able to cross the BBB. With this approach we identified
328 bepridil and beraprost as the two compounds which may bind specifically at the catalytic site
329 of TLK1 receptor protein and also fulfilled the CNS drugs selection criteria (Jeffrey, &
330 Summerfield 2010; Pardridge 1998). We observed that more than 80% of the interactions

331 involved between ligands and receptor are hydrophobic. We have also identified other lead
332 compounds for TLK1 such as the imidazole-pyrrole polyamide derivatives with better binding
333 affinity (with Moldock Score of -208.44 to -209.34) compared to bepridil and beraprost.
334 Unfortunately, these compounds violated the Lipinski's Rule of Five and have molecular
335 masses of more than 450 Da which are not suitable to cross the blood brain barrier.

336

337 Beraprost, an analogue to prostacyclin or PGI₂, is commonly used for arterial pulmonary
338 hypertension and has multiple physiological effects such as endothelial vasodilation, inhibition
339 of platelet aggregation, leukocyte adhesion, and vascular smooth muscle cell proliferation
340 (Wang et al. 2011). Activation of the PGI₂ signalling pathway by beraprost sodium suppressed
341 lung cancer metastases by preventing maturation of angiogenesis (Yoshinori Minami et al.
342 2012). It was also reported to enhance permeability and retention (EPR) of solid tumors by
343 decreasing tumor blood flow by 70%, hence inhibiting tumor growth. Moreover, it did not affect
344 normal cells and systemic blood flow (Tanaka et al. 2003). Since this compound mimics
345 structurally related lipid soluble hormone PGI₂, it was predicted that the efficacy of the
346 compound will be high as it will be able to cross the BBB (Moga 2013).

347

348 Bepridil is a known sodium-calcium channel blocker that is use for anti-arrythmias. An earlier
349 study reported that bepridil caused tumor growth inhibition in neuroblastoma and astrocytoma
350 cells by causing a prolonged increase in free intracellular calcium concentration when cells
351 were co-treated with anti-estrogens (Yong, & Wurster 1996). Bepridil has been experimentally
352 found to bind to the N-domain pocket of cardiac troponin C but with negative cooperativity
353 (Varguhese, & Li 2011). Even though, theoretically, bepridil can cross blood brain barrier
354 effectively (Muehlbacher et al. 2012), our findings showed that it may have non-specific

355 binding properties towards TLK1. Hence, it will be an added value if some chemical
356 modification can be made to increase its selectivity towards TLK1. It is worth to note that S-
357 bepridil was found to have a higher binding affinity towards the p53 binding domain in MDM2
358 (Warner et al. 2012). In order to enhance binding affinity between TLK1 receptor and these
359 two identified ligands, as well as preventing cross binding towards other types of receptors,
360 modification of current ligand structure by QSAR fragment based on pharmacophore analysis
361 is warranted for future study.

362

363 This study has identified potential inhibitors that binds at the catalytic site of TLK1. However,
364 identification of inhibitors that can bind to the non-catalytic component of a particular kinase
365 would also be useful as they would also play significant roles in the regulation of cellular
366 functions (Romano, & Kolch 2011). Further studies of TLK-ligand complex structure will
367 allow identification of allosteric inhibition sites to provide much specific TLK1 regulatory
368 inhibitory effects.

369

370 **Conclusion**

371 We have successfully created a 3D structure for the catalytic domain for TLK1 which was
372 predicted to be a potential molecular target for GBM. We have performed vigorous analysis to
373 determine the suitability and stability of the modelled structure through various quality control
374 platforms. We identified beraprost and bepridil as the two candidate compounds that will bind
375 to TLK1. These two drugs are commonly used for cardiovascular diseases. Further *in vitro* and
376 *in vivo* studies need to be performed to validate the therapeutic value of these compounds for
377 GBM.

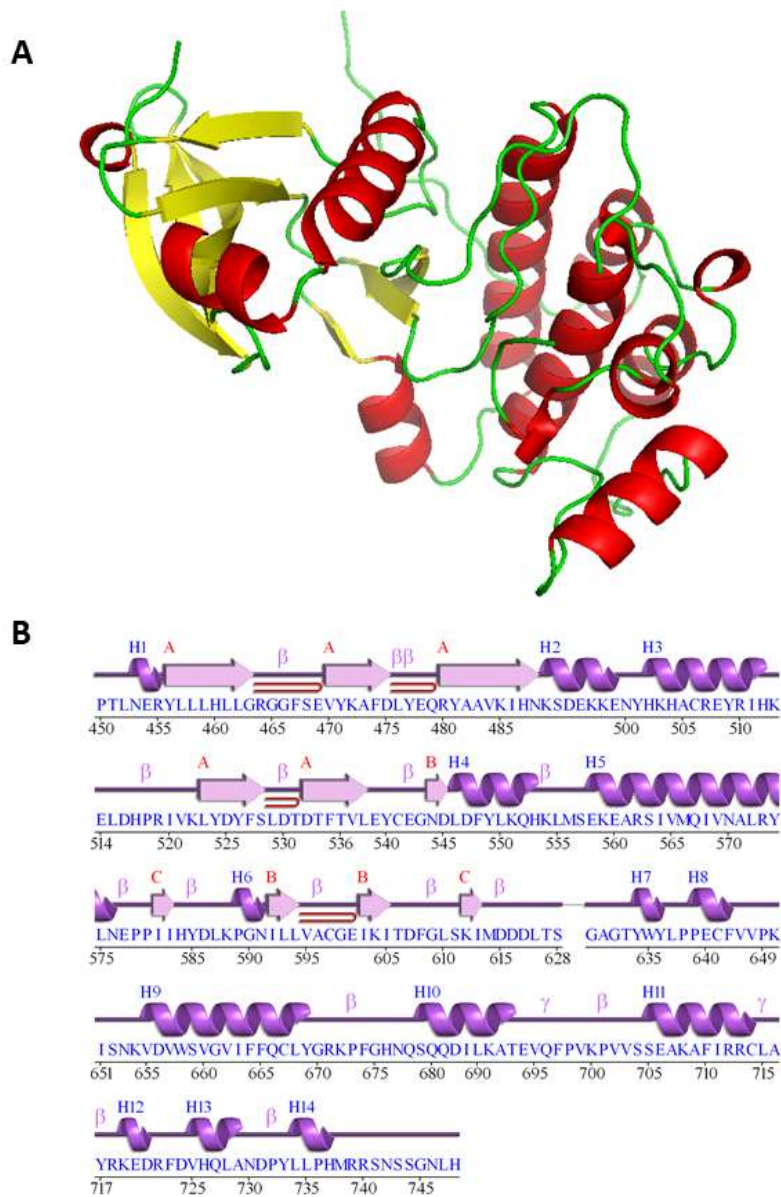
378

379 **Figures and Tables**

380 **Table 1:** Top 20 models generated from two homology modelling servers; Homology modeller
 381 (HOMER) and i-Tasser. TLK1homer4B8M was selected as our homology model for
 382 subsequent analysis.

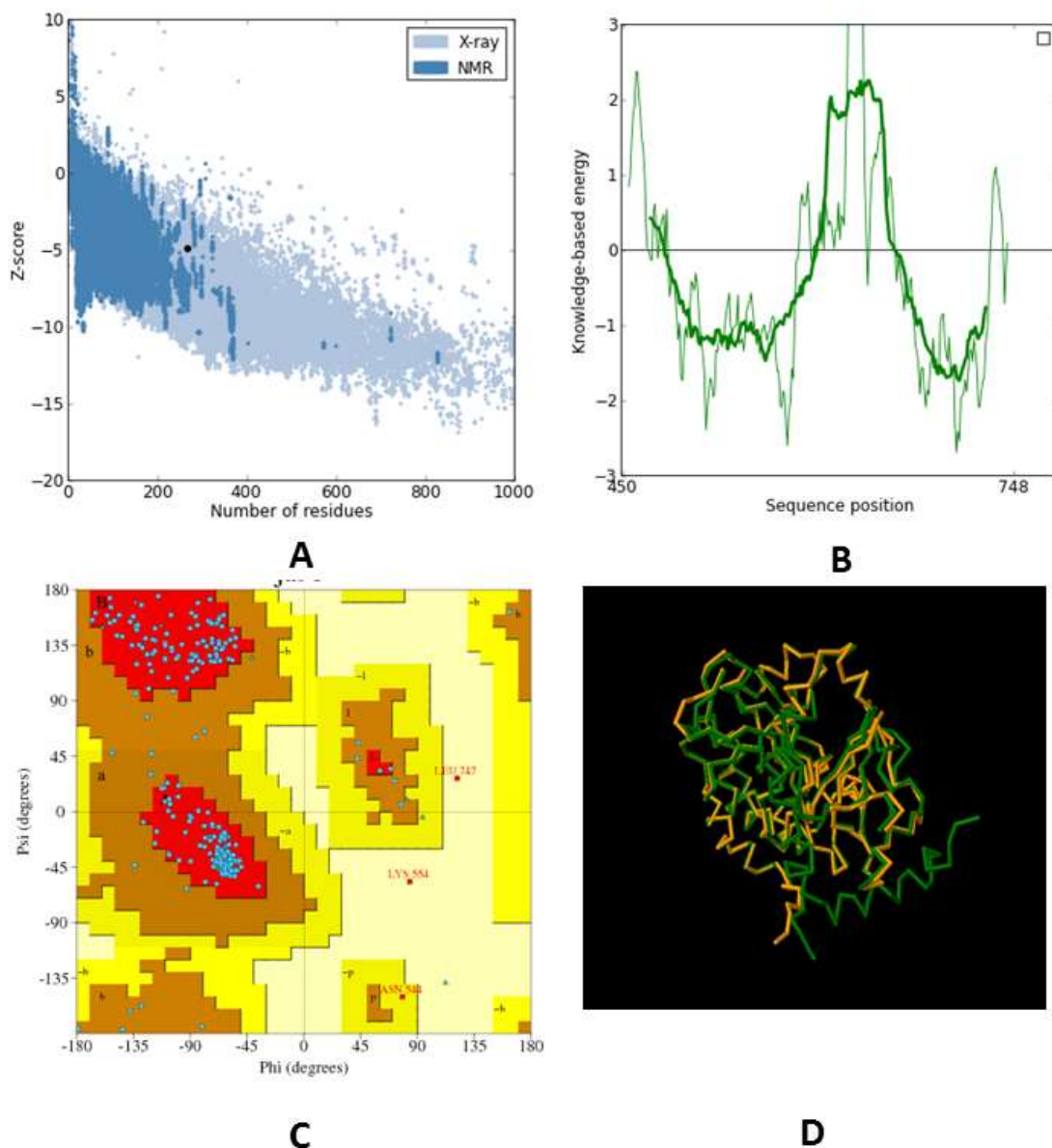
Model name	C_beta interaction energy	All-atom pairwise energy	Solvation energy	Torsion angle energy	Secondary structure agreement	Solvent accessibility agreement	Total QMEAN- score
TLK1homer4B8M	-61	-5727.18	-16.37	-16.13	89.30%	79.30%	0.68
TLK1homer4FR4	-74.72	6094.74	-11.26	-17.32	85.70%	77.60%	0.648
TLK1homer4DFX	-54.53	-6539.34	-22.18	-20.69	85.90%	77.10%	0.634
TLK1homer3SOA	-45.31	-5046.76	-4.80	-0.19	81.20%	78.80%	0.625
TLK1homer4M7N	-89.83	-5128.66	-15.31	-0.89	80.80%	79.10%	0.617
TLK1homer4FGB	-79.38	-6276.79	-16.15	-14.23	79.30%	77.50%	0.61
TLK1homer4L44m	-62.07	4967.85	-8.67	-4.86	86.60%	75.60%	0.604
TLK1homer3Q5I	-67.53	5211.28	-3.89	-6.1	77.20%	77.20%	0.596
TLK1homer4KIKB	-46.22	-3504.47	-4.66	-7.84	74.80%	77.20%	0.585
TLK1homer3TAC	-67.15	-5787.83	-12.33	5.77	81.70%	76.90%	0.582
TLK1homer1KOB	-67.51	-5454.16	-17.93	10.78	80.30%	77.30%	0.566
TLK1homer2Y94	-88.61	-5646.09	-14.67	13.09	81.40%	76.30%	0.558
TLK1homer2YCF	-71.96	-5698.7	-1.22	0.66	76.90%	74.40%	0.551
TLK1homer4EQC	-44.07	-5230.6	-15.55	0.2	79.40%	72.60%	0.511
TLK1homer3ZDU	-20.33	-3543.81	6.09	0.85	79.50%	70.90%	0.509
TLK1homer2ETR	-57.27	-5573.2	-12.92	-18.61	76.30%	68.60%	0.471
TLK1homer4FIE	-48.17	-4413.68	-7.96	-12.1	79.60%	78.60%	0.471
TLK1homer3I6U	-75.46	-6091.17	-6.14	4.72	68.40%	70.50%	0.443
tlk1model2itasser	-211.76	-9701.51	-35.09	43.13	77.80%	65.40%	0.371
tlk1model1itasser	-114.9	-6928.17	-22.73	29.02	71.00%	61.60%	0.294

383



384

385 **Figure 1:** (A) Secondary structure of TLK1 homology model generated from Homology
 386 Modeller server. Visualization was performed using The PyMOL Molecular Graphics System,
 387 Version 1.5.0.4 Schrödinger, LLC.; b-sheets, alpha-helices and loops are in yellow, red and
 388 green respectively. (B) Depiction of the amino acid residues that used in secondary structure
 389 analysed from Pro-Motif analysis using PDBsum server.



390

391 **Figure 2:** (A) ProSA shows the overall quality model of TLK1 with score of -4.92 (B) ProSA
 392 comparison results of energy-plots for TLK1 model structure with the PDB ID: 4B8M. (C)
 393 Ramachandran plot analysis using PROCHECK shows 90.1% of amino acids are generously
 394 in the allowed region. (D) 3D structural superposition of Aurora B kinase (PDB ID:4B8M)
 395 (green) and homology model of TLK1 (yellow).

396

397

398 **Table 2:** Ramachandran plot statistics of TLK1 homology model structure obtained from
399 PROCHECK analysis.

Parameter	Value in percentage
Most favoured region	90.1
Additional allowed region	8.7
Generously allowed region	0.4
Disallowed region	0.8
Amino acid residues accepted in the analysis	242 out of 270
G-factor average score	0.22
Main chain bond angles	0.41
Main chain bond lengths	0.62

400

401

402

403

404

405

406

407 **Table 3:** Lead molecules with their docking scores and amino acids interaction identified. In
 408 bold, are common residues that involved in the ATP, Befaprost and Beraprost binding.

409

Lead molecules ID	Chemical name	MolDock Score	Rerank Score	H-Bond score	Amino acids involved in interaction
352	Befaprost	-170.518	-109.678	-2.5	GLY465, GLY466, PHE467, SER468, VAL470, LYS485, HIS487, GLU496, TYR501, HIS502, HIS504, ALA505, TYR509, GLU508, HIS512, LEU523, THR536, LEU538, THR606, ASP607, PHE608,
1652	Befaprost/ Beraprost	-181.124	37.981	-5.35	GLY465, GLY466, PHE467, SER468, VAL470, LYS485, HIS487, GLU496, TYR501, HIS502, HIS504, ALA505, CYS506, TYR509, SER528, THR533
*367 (Control)	ATP	-186.431	-49.1549	-9.386	GLY463, ARG464, GLY465, GLY466, PHE467, SER468, GLU469, VAL470, LYS485

410

411

412 **Table 4:** Physiochemical properties of ligands from the docking study that passes ADME-TOX

413 Lipinski rule of five and CNS filtering.

Parameters	ID352	ID1652
MW	366.54	402.52
logP	5.31	4.1
logSw	-4.94	-4.33
tPSA	16.91	89.52
Rotatable bonds	10	10
Rigid Bonds	17	16
Flexibility	0.37	0.38
HB Donors	0	3
HB Acceptors	3	5
HBD_HBA	3	8
Number of system ring	3	1
Max Size System Ring	6	12
Charge	1	1
Total charge	1	-1
Heavy atoms	27	29
C atoms	24	24
Heteroatoms	3	5
Ratio H/C	0.12	0.21
Lipinski violation	1	0
Solubility mg/ml	2613.49	5304.9
Solubility forecast index	Reduced solubility	Reduced solubility
Phospholipidosis	Non-inducer	Non-inducer
Stereocenters	1	6
iPPI	No	No
Status	Accepted	Accepted

414

415

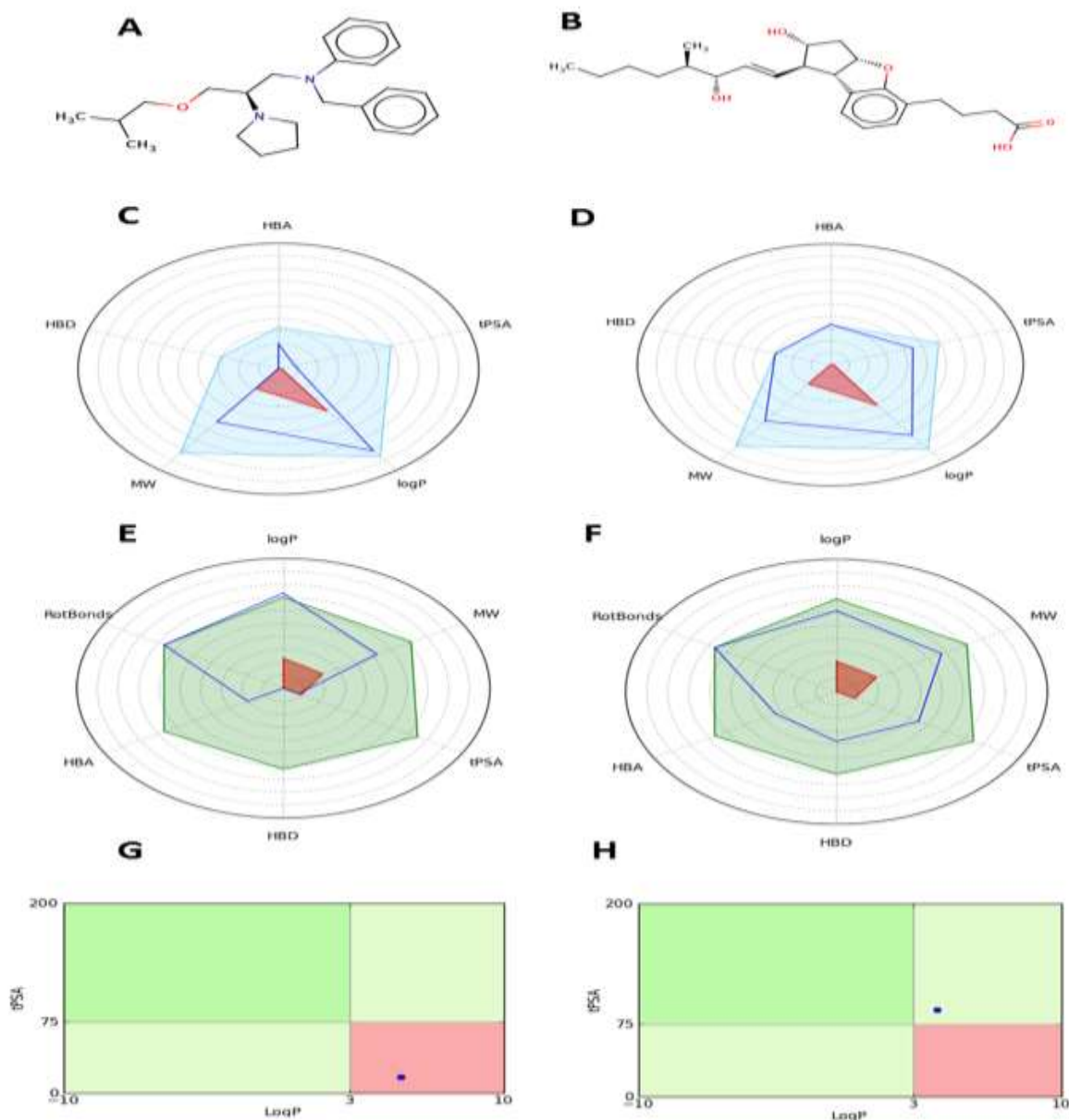
416

417

418

419

420



421

422 **Figure 3:** (A) and (B) Structure of identified compounds ID352; *N*-benzyl-*N*-(3-isobutoxy-2-
 423 *pyrrolidin-1-yl-propyl)aniline* and ID1652; *2,3,3a,8b-tetrahydro-2-hydroxy-1-(3-hydroxy-4-*
 424 *methyl-1-octen-6-ynyl)-1H-cyclopenta(b)benzofuran-5-butanoic acid* respectively. (C) and
 425 (D) Physico-chemical profile of compounds ID352 and ID1652, respectively. A radar plot
 426 representing the computed compound profile blue line that should cover within the CNS filter
 427 area in red and must be within the blue field. (E) and (F) Oral absorption estimation of ID352
 428 and ID1652, whereby the compound values should fall within RO5 and Veber rule area; light

429 green and red area. **(G)** and **(H)** Shows oral bioavailability profile (compound blue dot should
430 fall within the optimal dark green and light green area and red ones being extreme zones
431 generally indicating low oral bioavailability). ID352 were predicted to cause toxicity compared
432 to ID1652 whereby dot plot falls within the green area which is less likely to cause toxicity.

433

434

435

436

437

438

439

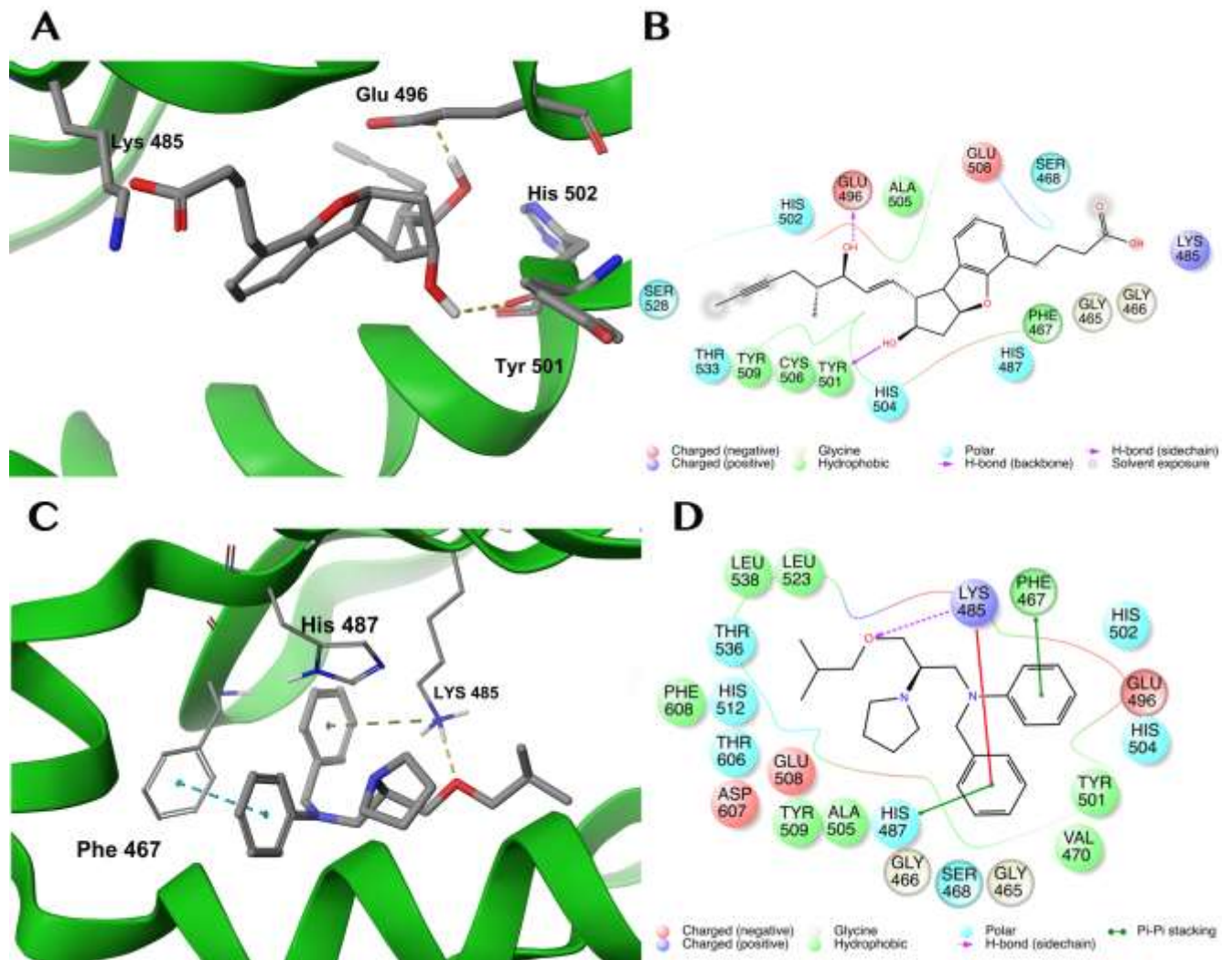
440

441

442

443

444



445

446

447 **Figure 4:** (A) 3D binding mode of the ligands ID1652 in the ATP binding site of the homology
 448 modeled TLK1 protein. The docking pose between ligand 1652 and the ATP binding site of
 449 TLK1 protein shows two backbone hydrogen bonds between the ligand and TYR501 and
 450 GLU496. (B) 2D ligand interaction diagram showing presence of hydrophobic interactions
 451 between the ligand and PHE467, ALA505, TRY501, CYS506 and TYR509. (C) 3D docking
 452 pose between ligand 352 and the ATP binding site of TLK1 showing an aromatic-aromatic and
 453 amino-aromatic interactions between the ligands and PHE467 and HIS487 respectively. There
 454 is also a hydrogen bond between the ligand and the LYS485. (D) 2D ligand interaction diagram
 455 showing hydrophobic interactions between the ligand and LEU523, LEU538, VAL470,

456 PHE467, TYR501, TYR509, ALA505 and PHE608. The fact that ligand ID1652 has more
457 activity than ligand 353 demonstrated the importance of hydrogen bonding rather than the
458 aromatic-aromatic and amino-aromatic interactions. Visualization of ligand-protein
459 interaction. The three-dimensional and two-dimensional visualisation of ligand-protein
460 interaction were performed using Maestro software package (Maestro, version 10.4,
461 Schrödinger, LLC, New York, NY, 2015).

462

463

464

465

466

467

468

469

470

471

472

473

474

475

476

477 **References**

- 478 Baker, G. J., Yadav, V. N., Motsch, S., Koschmann, C., Calinescu, A.-A., Mineharu, Y.,
479 Camelo-Piragua, S. I. et al. 2014. Mechanisms of glioma formation: iterative
480 perivascular glioma growth and invasion leads to tumor progression, VEGF-independent
481 vascularization, and resistance to antiangiogenic therapy. *Neoplasia (New York, N.Y.)*,
482 16(7), 543–561. doi:10.1016/j.neo.2014.06.003
- 483 Benkert, P., Biasini, M. & Schwede, T. 2011. Toward the estimation of the absolute quality
484 of individual protein structure models. *Bioinformatics (Oxford, England)*, 27(3), 343–
485 350. doi:10.1093/bioinformatics/btq662
- 486 Benkert, P., Tosatto, S. C. E. & Schomburg, D. 2008. QMEAN: A comprehensive scoring
487 function for model quality assessment. *Proteins: Structure, Function, and*
488 *Bioinformatics*, 71(1), 261–277.
- 489 Bento, A. P., Gaulton, A., Hersey, A., Bellis, L. J., Chambers, J., Davies, M., Krüger, F. A. et
490 al. 2014. The ChEMBL bioactivity database: an update. *Nucleic acids research*,
491 42(Database issue), D1083–90.
- 492 Brylinski, M. & Skolnick, J. 2008. A threading-based method (FINDSITE) for ligand-binding
493 site prediction and functional annotation. *Proceedings of the National Academy of*
494 *Sciences of the United States of America*, 105(1), 129–134.
495 doi:10.1073/pnas.0707684105
- 496 Buchan, D. W. A., Ward, S. M., Lobley, A. E., Nugent, T. C. O., Bryson, K. & Jones, D. T.
497 2010. Protein annotation and modelling servers at University College London 38(May),
498 563–568. doi:10.1093/nar/gkq427
- 499 Carrera, P., Moshkin, Y. M., Gronke, S., Sillje, H. H. W., Nigg, E. A., Jackle, H. & Karch, F.
500 2003. Tousled-like kinase functions with the chromatin assembly pathway regulating
501 nuclear divisions. *Genes & development*, 17(20), 2578–2590. doi:10.1101/gad.276703
- 502 De Benedetti, A. 2012. The Tousled-Like Kinases as Guardians of Genome Integrity. *ISRN*
503 *molecular biology*, 2012, 627596.
- 504 Galiè, N., Humbert, M., Vachiéry, J.-L., Vizza, C. D., Kneussl, M., Manes, A., Sitbon, O. et
505 al. 2002. Effects of beraprost sodium, an oral prostacyclin analogue, in patients with
506 pulmonary arterial hypertension: a randomized, double-blind, placebo-controlled trial.
507 *Journal of the American College of Cardiology*, 39(9), 1496–1502.
- 508 Garrote, A. M., Redondo, P., Montoya, G. & Muñoz, I. G. 2014. Purification, crystallization
509 and preliminary X-ray diffraction analysis of the kinase domain of human tousled-like
510 kinase 2. *Acta crystallographica. Section F, Structural biology communications*, 70(Pt
511 3), 354–357.
- 512 Gidda, J. S., Evans, D. C., Cohen, M. L., Wong, D. T., Robertson, D. W. & Parli, C. J. 1995.
513 Antagonism of serotonin₃ (5-HT₃) receptors within the blood-brain barrier prevents
514 cisplatin-induced emesis in dogs. *The Journal of pharmacology and experimental*
515 *therapeutics*, 273(2), 695–701.
- 516 Groth, A., Lukas, J., Nigg, E. a., Silljé, H. H. W., Wernstedt, C., Bartek, J. & Hansen, K.
517 2003. Human Tousled like kinases are targeted by an ATM- and Chk1-dependent DNA
518 damage checkpoint. *EMBO Journal*, 22(7), 1676–1687. doi:10.1093/emboj/cdg151

- 519 Guvenc, H., Pavlyukov, M. S., Joshi, K., Kurt, H., Banasavadi-Siddegowda, Y. K., Mao, P.,
520 Hong, C. et al. 2013. Impairment of glioma stem cell survival and growth by a novel
521 inhibitor for Survivin-Ran protein complex. *Clinical cancer research : an official*
522 *journal of the American Association for Cancer Research*, 19(3), 631–642.
523 doi:10.1158/1078-0432.CCR-12-0647
- 524 Ibrahim, K., Mat, F. C., Harun, R., Ngah, W. Z. W., Mokhtar, N. M. & Jamal, R. 2013.
525 Silencing of Tausled-like Kinase 1 (TLK1) Reduces Survival, Migration and Invasion of
526 Glioblastoma multiforme cells. *Asia Pacific Journal of Molecular Medicine*, 41(1st
527 National Conference for Cancer Research 5th Regional Conference on Molecular
528 Medicine RCMM).
- 529 Jeffrey, P. & Summerfield, S. 2010. Assessment of the blood-brain barrier in CNS drug
530 discovery. *Neurobiology of disease*, 37(1), 33–37. doi:10.1016/j.nbd.2009.07.033
- 531 Kelly, R. & Davey, S. K. 2013. Tausled-like kinase-dependent phosphorylation of Rad9
532 plays a role in cell cycle progression and G2/M checkpoint exit. *PLoS one*, 8(12),
533 e85859. doi:10.1371/journal.pone.0085859
- 534 Li, Q. & Tu, Y. 2015. Genetic Characteristics of Glioblastoma: Clinical Implications of
535 Heterogeneity. *Cancer Translational Medicine*, 1(5), 176. doi:10.4103/2395-
536 3977.168573
- 537 Li, Y., DeFatta, R., Anthony, C., Sunavala, G. & De Benedetti, A. 2001. A translationally
538 regulated Tausled kinase phosphorylates histone H3 and confers radioresistance when
539 overexpressed. *Oncogene*, 20(6), 726–738. doi:10.1038/sj.onc.1204147
- 540 Lipinski, C. A., Lombardo, F., Dominy, B. W. & Feeney, P. J. 2001. Experimental and
541 computational approaches to estimate solubility and permeability in drug discovery and
542 development settings. *Advanced drug delivery reviews*, 46(1-3), 3–26.
- 543 Miteva, M. A., Violas, S., Montes, M., Gomez, D., Tuffery, P. & Villoutreix, B. O. 2006.
544 FAF-Drugs: free ADME/tox filtering of compound collections. *Nucleic acids research*,
545 34(Web Server issue), W738–44. doi:10.1093/nar/gkl065
- 546 Moga, T. 2013. The 2-Series Eicosanoids in Cancer: Future Targets for Glioma Therapy?
547 *Journal of Cancer Therapy*. *Journal of Cancer Therapy*, 338–352 SRC – Google Scholar.
- 548 Muehlbacher, M., Tripal, P., Roas, F. & Kornhuber, J. 2012. Identification of Drugs Inducing
549 Phospholipidosis by Novel in vitro Data. *Chemmedchem*, 7(11), 1925–1934.
550 doi:10.1002/cmde.201200306
- 551 Nathanson, D. & Mischel, P. S. 2011. Charting the course across the blood-brain barrier. *The*
552 *Journal of clinical investigation*, 121(1), 31–33. doi:10.1172/JCI45758
- 553 Ohgaki, H., Dessen, P., Jourde, B., Horstmann, S., Nishikawa, T., Di Patre, P.-L., Burkhard,
554 C. et al. 2004. Genetic pathways to glioblastoma: a population-based study. *Cancer*
555 *research*, 64(19), 6892–6899. doi:10.1158/0008-5472.CAN-04-1337
- 556 Ohgaki, H. & Kleihues, P. 2007. Genetic pathways to primary and secondary glioblastoma.
557 *The American journal of pathology*, 170(5), 1445–1453.
558 doi:10.2353/ajpath.2007.070011
- 559 Ohgaki, H. & Kleihues, P. 2011. Genetic profile of astrocytic and oligodendroglial gliomas.
560 (1). *Brain tumor pathology*, 28(3), 177–183. doi:10.1007/s10014-011-0029-1

- 561 Pajouhesh, H. & Lenz, G. R. 2005. Medicinal chemical properties of successful central
562 nervous system drugs. *NeuroRx : the journal of the American Society for Experimental*
563 *NeuroTherapeutics*, 2(4), 541–553.
- 564 Pardridge, W. M. 1998. CNS drug design based on principles of blood-brain barrier transport.
565 *Journal of neurochemistry*, 70(5), 1781–1792.
- 566 Piccirillo, S. G. M., Spiteri, I., Sottoriva, A., Touloumis, A., Ber, S., Price, S. J., Heywood, R.
567 et al. 2015. Contributions to Drug Resistance in Glioblastoma Derived from Malignant
568 Cells in the Sub- Ependymal Zone 2004(10), 194–203. doi:10.1158/0008-5472.CAN-
569 13-3131
- 570 Pilyugin, M., Demmers, J., Verrijzer, C. P., Karch, F. & Moshkin, Y. M. 2009.
571 Phosphorylation-mediated control of histone chaperone ASF1 levels by Tausled-like
572 kinases. *PloS one*, 4(12), e8328. doi:10.1371/journal.pone.0008328
- 573 Pruitt, K. D., Tatusova, T., Brown, G. R. & Maglott, D. R. 2012. NCBI Reference Sequences
574 (RefSeq): current status, new features and genome annotation policy. *Nucleic acids*
575 *research*, 40(Database issue), D130–5. doi:10.1093/nar/gkr1079
- 576 Rae, A. P., Beattie, J. M., Lawrie, T. D. & Hutton, I. 1985. Comparative clinical efficacy of
577 bepridil, propranolol and placebo in patients with chronic stable angina. *British journal*
578 *of clinical pharmacology*, 19(3), 343–352.
- 579 Romano, J. D. & Kolch, W. 2011. The secret life of kinases functions beyond catalysis. *Cell*
580 *Communication Signalling*
- 581 Ronald, S., Awate, S., Rath, A., Carroll, J., Galiano, F., Kleiner-hancock, H., Mathis, J. M. et
582 al. 2013. Phenothiazine Inhibitors of TLKs Affect Double-Strand Break Repair and
583 DNA Damage Response Recovery and Potentiate Tumor Killing with Radiomimetic
584 Therapy. doi:10.1177/1947601913479020
- 585 Ronald, S., Sunavala-Dossabhoj, G., Adams, L., Williams, B. & De Benedetti, A. 2011. The
586 expression of Tausled kinases in CaP cell lines and its relation to radiation response and
587 DSB repair. *The Prostate*, 71(13), 1367–1373. doi:10.1002/pros.21358
- 588 Ruano, Y., Mollejo, M., Camacho, F. I., de Lope, A., Fiaño, C., Ribalta, T., Martínez, P. et al.
589 2008. Identification of survival-related genes of the phosphatidylinositol 3'-kinase
590 signaling pathway in glioblastoma multiforme. *Cancer*, 112(7), 1575–1584.
591 doi:10.1002/cncr.23338
- 592 Sangar, V., Funk, C. C., Kusebauch, U., Campbell, D. S., Moritz, R. L. & Price, N. D. 2014.
593 Quantitative proteomic analysis reveals effects of epidermal growth factor receptor
594 (EGFR) on invasion-promoting proteins secreted by glioblastoma cells. *Molecular &*
595 *cellular proteomics : MCP*, 13(10), 2618–2631. doi:10.1074/mcp.M114.040428
- 596 Silljé, H. H., Takahashi, K., Tanaka, K., Van Houwe, G. & Nigg, E. A. 1999. Mammalian
597 homologues of the plant Tausled gene code for cell-cycle-regulated kinases with
598 maximal activities linked to ongoing DNA replication. *The EMBO journal*, 18(20),
599 5691–5702. doi:10.1093/emboj/18.20.5691
- 600 Sivaprakasam, P., Tosso, P. N. & Doerksen, R. J. 2009. Structure-activity relationship and
601 comparative docking studies for cycloguanil analogs as PfdHFR-TS inhibitors. *Journal*
602 *of chemical information and modeling*, 49(7), 1787–1796. doi:10.1021/ci9000663
- 603 Smith, J. S., Tachibana, I., Passe, S. M., Huntley, B. K., Borell, T. J., Iturria, N., O'Fallon, J.

- 604 R. et al. 2001. PTEN mutation, EGFR amplification, and outcome in patients with
605 anaplastic astrocytoma and glioblastoma multiforme. *Journal of the National Cancer*
606 *Institute*, 93(16), 1246–1256.
- 607 Sumathi, K., Ananthalakshmi, P., Roshan, Mnam. & Sekar, K. 2006. 3dSS: 3D structural
608 superposition. *Nucleic Acids Research*, 34, W128–W132.
- 609 Sunavala-Dossabhoy, G. & De Benedetti, A. 2009. Tousled homolog, TLK1, binds and
610 phosphorylates Rad9; TLK1 acts as a molecular chaperone in DNA repair. *DNA repair*,
611 8(1), 87–102. doi:10.1016/j.dnarep.2008.09.005
- 612 Sundarapandian, T., Shalini, J., Sugunadevi, S. & Woo, L. K. 2010. Journal of Molecular
613 Graphics and Modelling Docking-enabled pharmacophore model for histone deacetylase
614 8 inhibitors and its application in anti-cancer drug discovery. *Journal of Molecular*
615 *Graphics and Modelling*, 29(3), 382–395. doi:10.1016/j.jmgs.2010.07.007
- 616 Takahata, S., Yu, Y. & Stillman, D. J. 2009. The E2F functional analogue SBF recruits the
617 Rpd3(L) HDAC, via Whi5 and Stb1, and the FACT chromatin reorganizer, to yeast G1
618 cyclin promoters. *The EMBO journal*, 28(21), 3378–3389. doi:10.1038/emboj.2009.270
- 619 Takayama, Y., Kokuryo, T., Yokoyama, Y., Ito, S., Nagino, M., Hamaguchi, M. & Senga, T.
620 2010. Silencing of Tousled-like kinase 1 sensitizes cholangiocarcinoma cells to
621 cisplatin-induced apoptosis. *Cancer letters*, 296(1), 27–34.
622 doi:10.1016/j.canlet.2010.03.011
- 623 Tanaka, S., Akaike, T., Wu, J., Fang, J., Sawa, T., Ogawa, M., Beppu, T. et al. 2003.
624 Modulation of tumor-selective vascular blood flow and extravasation by the stable
625 prostaglandin 12 analogue beraprost sodium. *Journal of drug targeting*, 11(1), 45–52.
- 626 Tosatto, S. C. E. 2005. The victor/FRST function for model quality estimation. *Journal of*
627 *computational biology : a journal of computational molecular cell biology*, 12(10),
628 1316–1327. doi:10.1089/cmb.2005.12.1316
- 629 Tung, C.-H., Huang, J.-W. & Yang, J.-M. 2007. Kappa-alpha plot derived structural alphabet
630 and BLOSUM-like substitution matrix for rapid search of protein structure database.
631 *Genome biology*, 8(3), R31. doi:10.1186/gb-2007-8-3-r31
- 632 Varguhese, J. F. & Li, Y. 2011. Molecular dynamics and docking studies on cardiac troponin
633 C. *Journal of biomolecular structure & dynamics*, 29(1), 123–135.
- 634 von Grotthuss, M., Pas, J. & Rychlewski, L. 2003. Ligand-Info, searching for similar small
635 compounds using index profiles. *Bioinformatics (Oxford, England)*, 19(8), 1041–1042.
- 636 Wang, J., Zhang, J., Sun, J., Han, J., Xi, Y., Wu, G., Duan, K. X. et al. 2011. Prostacyclin
637 administration as a beneficial supplement to the conventional cancer chemotherapy.
638 *Medical hypotheses*, 76(5), 695–696.
- 639 Warner, W. A., Sanchez, R., Dawoodian, A., Li, E. & Momand, J. 2012. Identification of
640 FDA-approved drugs that computationally bind to MDM2. *Chemical biology & drug*
641 *design*, 80(4), 631–637.
- 642 Wiederstein, M. & Sippl, M. J. 2007. ProSA-web: interactive web service for the recognition
643 of errors in three-dimensional structures of proteins. *Nucleic acids research*, 35(Web
644 Server issue), W407–10. doi:10.1093/nar/gkm290
- 645 Wolfort, R., de Benedetti, A., Nuthalapaty, S., Yu, H., Chu, Q. D. & Li, B. D. 2006. Up-

- 646 regulation of TLK1B by eIF4E overexpression predicts cancer recurrence in irradiated
647 patients with breast cancer. *Surgery*, 140(2), 161–169.
- 648 Yong, S. L. & Wurster, R. D. 1996. Bepiridil enhances in vitro antitumor activity of
649 antiestrogens in human brain tumor cells. *Cancer Lett*, 110 SRC - , 243–248.
- 650 Yoshinori Minami et al. 2012. Activating the prostaglandin I2-IP signaling suppresses
651 metastasis in lung cancer. *Cancer Research*, 4379(In Proceedings of the 103rd Annual
652 Meeting of the American Association for Cancer Research).
- 653 Zhang, Y. 2009. I-TASSER: Fully automated protein structure prediction in CASP8.
654 *Proteins: Structure, Function, and Bioinformatics*, 77, 100–113.
- 655